Research article

Modulation of L-type Ca^{2+} current but not activation of Ca^{2+} release by the gamma$_1$ subunit of the dihydropyridine receptor of skeletal muscle

Chris A Ahern[1,1], Patricia A Powers[2], Gloria H Biddlecome[3,4], Laura Roethe[2], Paola Vallejo[1], Lindsay Mortenson[1], Caroline Strube[5], Kevin P Campbell[3,4], Roberto Coronado[1] and Ronald G Gregg*[6]

Address: [1]Department of Physiology, University of Wisconsin School of Medicine, and, [2]Biotechnology Center, University of Wisconsin, Madison, WI, 53706, USA;, [3]Howard Hughes Medical Institute, and, [4]Departments of Physiology and Biophysics, and Neurology, The University of Iowa College of Medicine, Iowa City, IA, 52242, USA;, [5]Laboratoire de Physiologie des Elements Excitables, Universite Claude Bernard - Lyon 1, France; and and [6]Department of Biochemistry and Molecular Biology, and Department of Ophthalmology and Visual Sciences, University of Louisville, Louisville, KY, 40202, USA

E-mail: Chris A Ahern - cahern@physiology.wisc.edu; Patricia A Powers - papowers@facstaff.wisc.edu; Gloria H Biddlecome - gloriab@amgen.com; Laura Roethe - lroethe@facstaff.wisc.edu; Paola Vallejo - paolavalejo@hotmail.com; Lindsay Mortenson - lindsay@physiology.uiowa.edu; Caroline Strube - caroline.strube@univ-lyon1.fr; Kevin P Campbell - campbellk@physiology.uiowa.edu; Roberto Coronado - coronado@physiology.wisc.edu; Ronald G Gregg* - ron.gregg@louisville.edu

*Corresponding author

Published: 24 July 2001

BMC Physiology 2001, **1**:8

Received: 23 April 2001
Accepted: 24 July 2001

This article is available from: http://www.biomedcentral.com/1472-6793/1/8

Abstract

Background: The multisubunit (α_{1S},α_2-δ, β_{1a} and γ_1) skeletal muscle dihydropyridine receptor (DHPR) transduces membrane depolarization into release of Ca^{2+} from the sarcoplasmic reticulum (SR) and also acts as an L-type Ca^{2+} channel. To more fully investigate the function of the γ_1 subunit in these two processes, we produced mice lacking this subunit by gene targeting.

Results: Mice lacking the DHPR γ_1 subunit (γ_1 null) survive to adulthood, are fertile and have no obvious gross phenotypic abnormalities. The γ_1 subunit is expressed at approximately half the normal level in heterozygous mice (γ_1 het). The density of the L-type Ca^{2+} current in γ_1 null and γ_1 het myotubes was higher than in controls. Inactivation of the Ca^{2+} current produced by a long depolarization was slower and incomplete in γ_1 null and γ_1 het myotubes, and was shifted to a more positive potential than in controls. However, the half-activation potential of intramembrane charge movements was not shifted, and the maximum density of the total charge was unchanged. Also, no shift was observed in the voltage-dependence of Ca^{2+} transients. γ_1 null and γ_1 het myotubes had the same peak Ca^{2+} amplitude vs. voltage relationship as control myotubes.

Conclusions: The L-type Ca^{2+} channel function, but not the SR Ca^{2+} release triggering function of the skeletal muscle dihydropyridine receptor, is modulated by the γ_1 subunit.

Background

In skeletal muscle, the dihydropyridine receptor (DHPR) consists of α_{1S}, α_2-δ, β_{1a} and γ_1 subunits [1]. This complex is responsible for the L-type Ca^{2+} current and serves as

the voltage sensor for excitation-contraction (EC) coupling. In the latter process, the movement of electrical charges in the α_{1S} subunit promotes a conformational change that opens the ryanodine receptor type-1 (RyR1) in the sarcoplasmic reticulum membrane (SR) leading to an increase in cytosolic Ca^{2+} [2,3]. The functional interactions between the DHPR subunits necessary for opening the Ca^{2+} channel are only partially known. Further, the interactions between DHPR subunits and RyR1 also are incompletely understood. The α_1 subunit is a large protein that contains the basic functional elements of the L-type Ca^{2+} channel, including the Ca^{2+} selectivity, voltage-dependent gating, and sensitivity to dihydropyridines. The cytoplasmic loop between repeats II and III of the α_{1S} subunit interacts closely with RyR1 and is an important determinant of skeletal type EC coupling [4,5]. A region in the cytoplasmic loop between repeats I and II of the α_1 subunit, referred to as the AID [6], binds tightly with a 30 amino acid region on the β_1 subunit, referred to as the BID [7]. β subunits are ~ 55 to 65 kDa proteins essential for channel assembly and/or membrane targeting, as well as for modulation of channel kinetics [8]. The α_2-δ subunit is a highly glycosylated ~ 175 kDa protein formed by two disulfide-linked peptides encoded by the same gene. Transmembrane topology and functional analyses suggest the α_2-δ subunit is composed of a single transmembrane domain and a short cytoplasmic tail of only five residues [9,10]. Given this topology, the α_2-δ subunit is most likely to interact with the α_1 and/or the γ_1 subunits. The γ_1 subunit is a ~ 32 kDa skeletal muscle-specific protein with four presumptive transmembrane domains [11,12,13]. The transmembrane topology of the γ_1 subunit and the critical binding domains are unknown at this time.

EC coupling is initiated by voltage-dependent charge movements in the S4 segments of the DHPR α_{1S} subunit, whose expression is dependent on the presence of the β_{1a} subunit [14]. The C-terminus of the β_{1a} subunit has also been shown to be important in EC coupling, presumably by interaction with RyR1 [15]. The role of the α_2-δ subunit on skeletal EC coupling is unknown, but in heterologous expression systems it has been demonstrated to increase the amount of charge movement [16]. The role of the γ_1 subunit in Ca^{2+} channel function is of particular interest given the discovery of a second γ subunit, γ_2 or *stargazin*, which is expressed in neurons and is responsible for the *stargazer* mutation in mice [17]. Subsequently, several other γ subunit genes have been identified and shown to be expressed in brain and peripheral tissues [18,19]. In the present study we examined the role of the γ_1 subunit in L-type Ca^{2+} current and EC coupling in skeletal myotubes. Absence of the γ_1 subunit slows inactivation and produces a depolarizing shift in the Ca^{2+} current inactivation vs. voltage curve, in agreement with results from an independently produced γ_1 knockout mouse [20]. However, absence of γ_1 does not affect the voltage dependence or the magnitude of charge movements and Ca^{2+} transients. Overall, the γ_1 subunit appears to promote inhibition of the Ca^{2+} channel function of the skeletal DHPR. While this subunit is clearly non-essential for activation of the L-type Ca^{2+} channel and for triggering skeletal-type EC coupling, γ_1 appears to specifically modulate the Ca^{2+} channel function of the skeletal DHPR.

Results and Discussion

Inactivation of the DHPR γ_1 subunit by gene targeting

Gene targeting was used to replace the entire coding region of the γ_1 gene with the *neo* gene, as described in Materials and Methods (Fig. 1). Targeted ES cell clones were injected into C57Bl/6J blastocysts and chimeras obtained. After additional breeding, a line containing the γ_1 targeted allele was obtained. Fig. 1A shows Southern blots from DNA of control (+/+), γ_1 het (+/-) and γ_1 null (-/-) mice, after digestion with *Eco*RI and hybridization to probe 1. The γ_1 het and γ_1 null mice show the predicted 12.5 kb restriction fragment indicative of the targeted allele (Fig. 1B). Similarly for the Southern blot of DNA digested with *Hind*III and hybridized to probe 2, the γ_1 het and γ_1 null mice show the predicted 3.5 kb restriction fragment indicative of the targeted allele (Fig. 1C). The γ_1 het and γ_1 null mice have no visible abnormalities and are fertile. Western blots showing the expression of the DHPR subunits are shown in Fig 1D. The amount of the γ_1 subunit present in control, γ_1 het and γ_1 null samples as a function of total membrane protein was determined in two independent membrane preparations. These data indicate that the amount of γ_1 expression in membranes from γ_1 null muscle was not detectable above background (no primary antibody) as expected from the fact that the entire gene was deleted. In membranes isolated from the γ_1 het mice, the level of expression of the γ_1 subunit was 64% of control values for each of the two independent determinations, consistent with what might be expected from the loss of one allele. Whether there is compensation by increased expression of other γ subunits such as the γ_6 and γ_7 subunits, which were shown recently to be present in skeletal muscle by RT-PCR [19], or alteration of the amount of the other subunits remains to be determined in the future.

Increase in Ca^{2+} current density and decrease in inactivation in γ_1 null and γ_1 het myotubes

We examined the impact of the γ_1 null mutation on DHPR properties using electrophysiological techniques in primary cultures of skeletal myotubes derived from mouse embryos. Fig. 2A shows whole-cell Ca^{2+} currents in control, γ_1 het and γ_1 null myotubes in response to 500-ms depolarizing voltage steps from a holding poten-

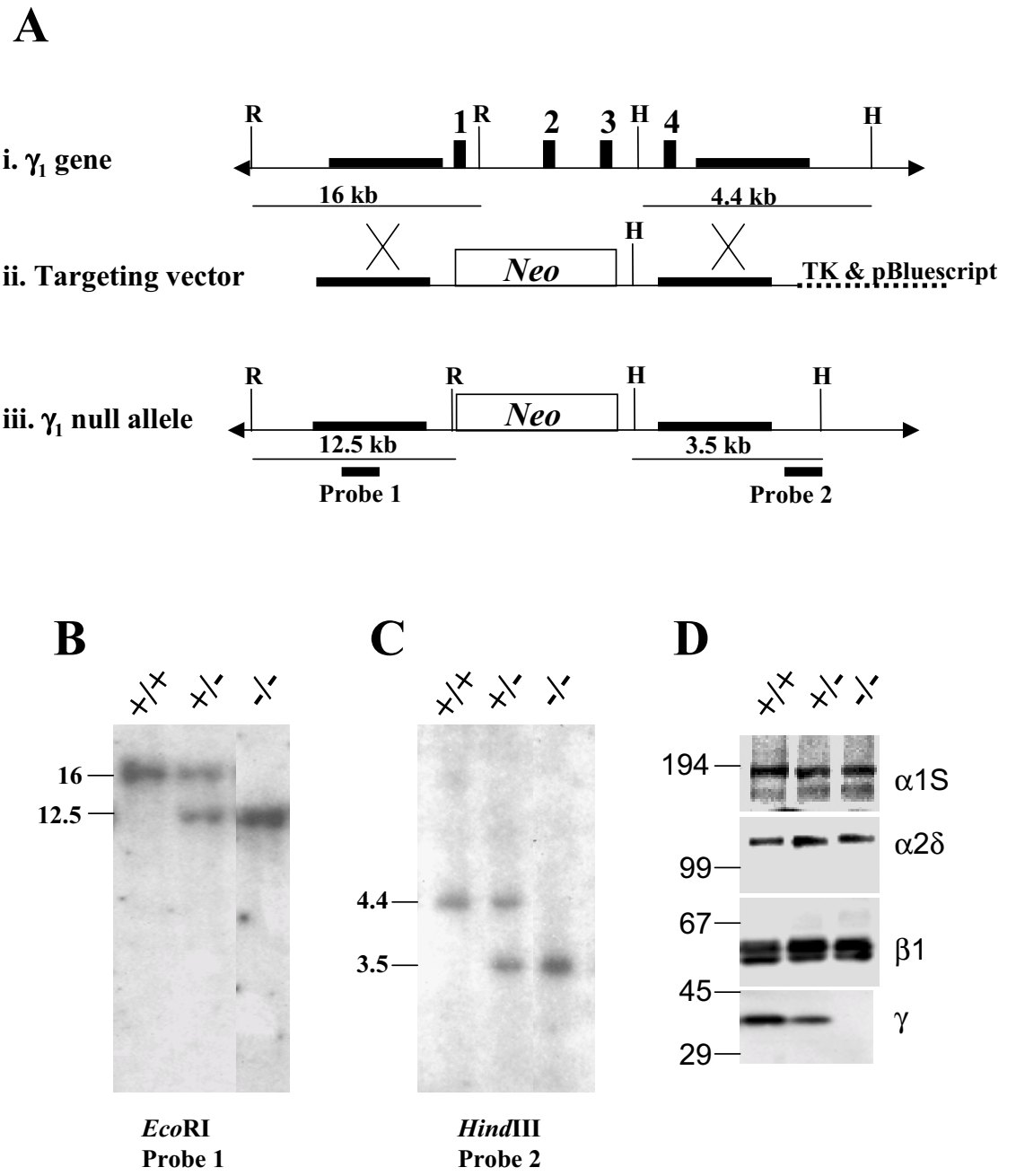

Figure 1

Inactivation of the γ_1 subunit by gene targeting. A) i. The normal γ_1 gene, which contains 4 exons (represented by black boxes). ii. The targeting vector contains a fragment with 4.4 kb of homology to a region 5' of exon 1 and a 2.6 kb fragment with homology to a region 3' of exon 4 (thick horizontal lines). These fragments are separated by the *neo* gene, which is used to select the ES cells in culture. iii. The modified γ_1 locus. When recombination occurs in the regions indicated by the X's, all 4 exons of the γ_1 gene are replaced by the *neo* cassette. B, C) Southern blots of DNA, either digested with *Eco*RI and hybridized to probe 1 (B), or DNA digested with *Hind*III and hybridized to probe 2 (C), from control (+/+), γ_1 het (+/-) and γ_1 null (-/-) mice. These data show the predicted size bands for the wild type and targeted alleles. D) Western blots for each of the four skeletal DHPR subunits from control (+/+), γ_1 het (+/-) and γ_1 null (-/-) mice. The γ_1 subunit is absent from the γ_1 null mice and at approximately half the normal level in the γ_1 het mice.

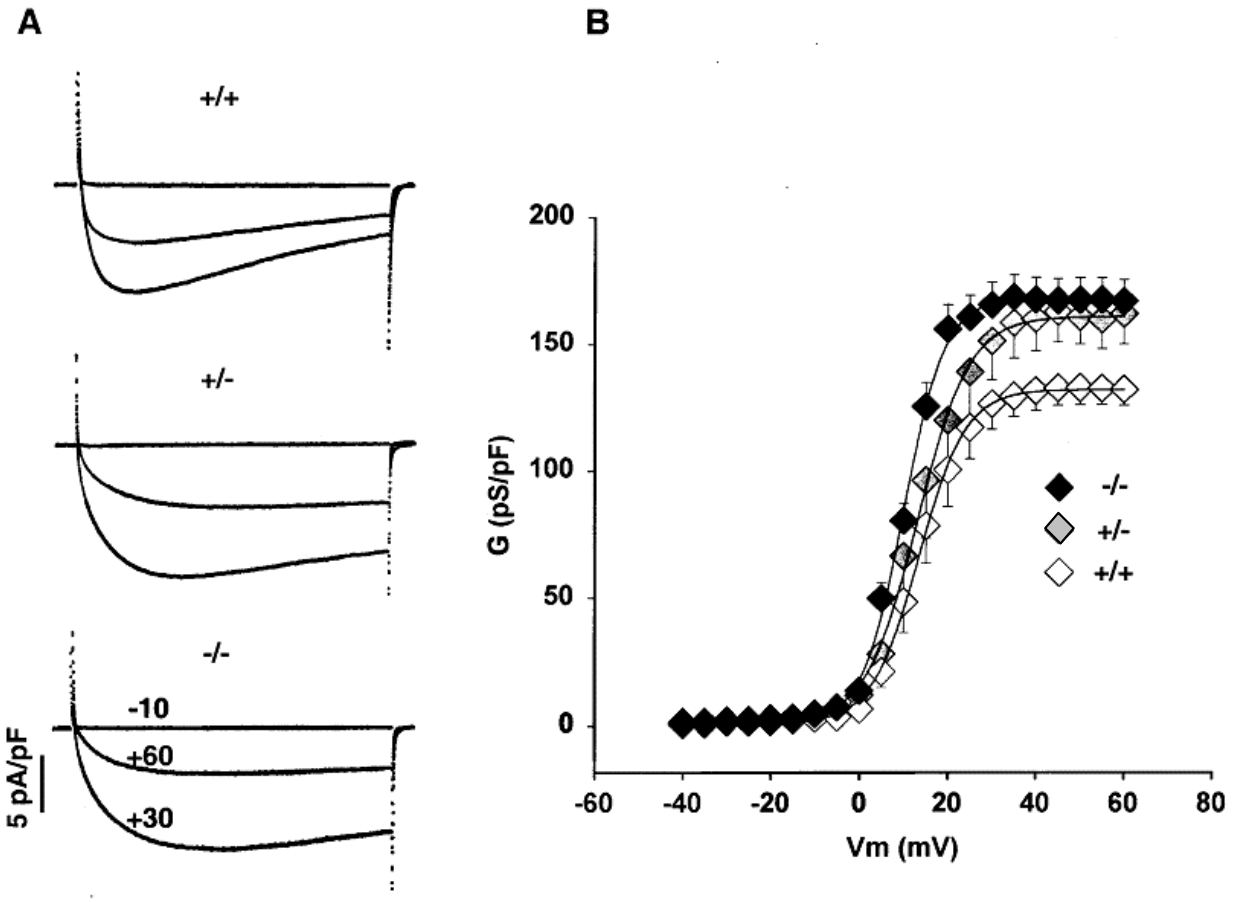

Figure 2

L-type Ca^{2+} conductance in γ_1 knockout myotubes. A) Whole-cell L-type Ca^{2+} current when control (+/+), γ_1 het (+/-), or γ_1 null (-/-) myotubes are depolarized to either -10 mV, +30 mV or +60 mV from a holding potential of -40 mV. The pulse duration was 500 ms. The cell capacitance was 262 pF, 221 pF, and 286 pF, for the control, γ_1 het and γ_1 null cells, respectively. B) Voltage dependence of the Ca^{2+} conductance for 8 control, 8 γ_1 het and 12 γ_1 null cells. The curves correspond to a Boltzmann fit of the population mean with the following parameters. G_{max} = 132 pS/pF, $V_{1/2}$ = 13.4 mV and k = 5.3 mV for control cells; G_{max} = 160 pS/pF, $V_{1/2}$ = 13 mV and k = 5.8 mV for γ_1 het cells; and G_{max} = 167 pS/pF, $V_{1/2}$ = 9.9 mV and k = 4.6 mV for γ_1 null cells.

tial of -40 mV. Current traces for only three voltage steps are shown for clarity. All three cell types displayed the slow, high-voltage activated L-type Ca^{2+} current typical of skeletal myotubes. When the holding potential was -80 mV, we also observed a T-type Ca^{2+} current, which was seen in approximately half of the cells tested (data not shown). Ca^{2+} conductance vs. voltage curves were computed in Fig. 2B for the three cell types. The sigmoidal lines correspond to a Boltzmann fit to the population mean while parameters fitted to each cell are shown in Table 1. These data show that the maximum conductance, G_{max}, for both the γ_1 het and γ_1 null cells are significantly larger ($p<0.05$) than the values for control cells. However, the half-activation potential ($V_{1/2}$) and the steepness of the curve (factor k) were not significantly different (see Table 1). Thus, full or partial elimination of the γ_1 subunit produced a significant increase in the Ca^{2+} current density without a change in the voltage-dependence of the Ca^{2+} conductance.

At intermediate potentials such as +30 mV (Fig. 2A), the Ca^{2+} current of γ_1 het and γ_1 null cells inactivated more slowly than that of control cells. To examine changes in inactivation, we used the paired-pulse protocol shown in Fig. 3A, which measured the Ca^{2+} current not inactivated by the pre-pulse. It has been shown that inactivation of

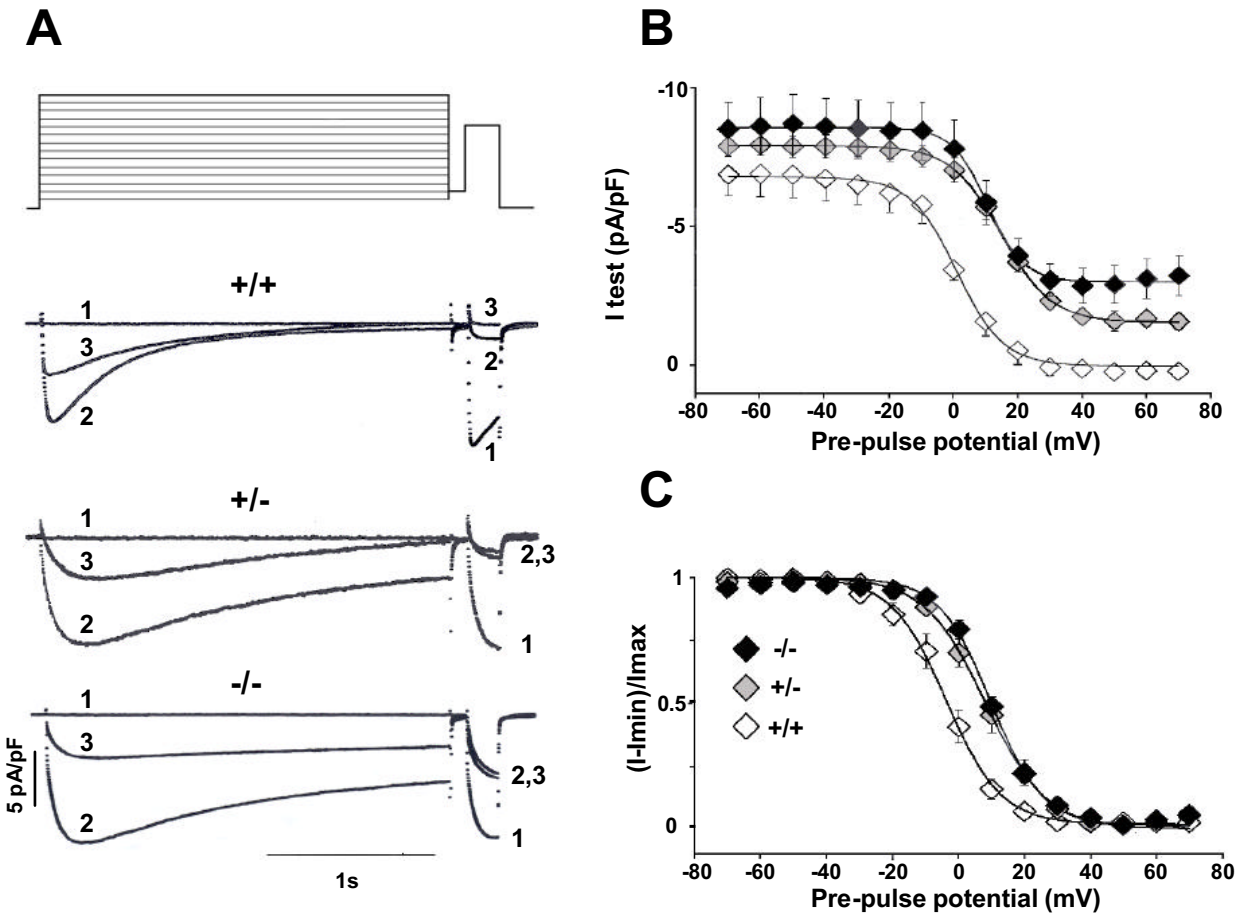

Figure 3

Slow inactivation of the Ca^{2+} current in γ_1 knockout myotubes. A) Diagram to scale of the two-pulse protocol used to inactivate the L-type Ca^{2+} current at each of 15 potentials and then the test potential (+20 mV) to measure the remaining non-inactivated current. Ca^{2+} currents during the pre-pulse and test-pulse phases of the protocol are shown for a pre-pulse depolarization to -70 mV (trace 1), +30 mV (trace 2) and +60 mV (trace 3) in a control, a γ_1 het, and a γ_1 null myotube. The cell capacitance was 317 pF for the control, 175 pF for the γ_1 het and 348 pF for the γ_1 null cell. B) The maximum Ca^{2+} current during the test pulse is plotted as a function of the pre-pulse potential for 6 control, 8 γ_1 het and 8 γ_1 null cells. C) The non-activating component was subtracted and the curves were normalized to show the voltage-dependence of the inactivating component. I is the maximum test current, Imin is the test current at +50 mV and Imax is the test current at -70 mV. The curves correspond to a Boltzmann fit of the population mean with the following parameters. $[(I-Imin)/Imax]_{max}$ = 1, $V_{1/2}$ = -3.8 mV and k = 8.4 mV for control cells. $[(I-Imin)/Imax]_{max}$ = 1, $V_{1/2}$ = +15.6 mV and k = 8.1 mV for γ_1 het cells. $[(I-Imin)/Imax]_{max}$ = 1, $V_{1/2}$ = +9.7 mV and k = 7.9 mV for γ_1 null cells.

skeletal L-type Ca^{2+} channels approaches steady-state extremely slowly, on the time scale of tens of seconds [21]. However, for comparative purposes and to be consistent with previous measurements in Ca^{2+} channels lacking γ_1 [20,22], we chose a much shorter protocol. Cells were held at -80 mV, then stepped to a series of depolarizing (pre-pulse) voltages for 2.5 s to promote inactivation, then stepped to -50 mV for 100 ms to close non-inactivated channels. The non-inactivated Ca^{2+} current was measured during a 200-ms test pulse to +20 mV. In control cells, there was almost complete inactivation of the Ca^{2+} current when the pre-pulse potential was in the positive range. This can be seen by comparing the amplitude of the Ca^{2+} current during the test pulse in traces 1, 2, and 3, corresponding to pre-pulse potentials to -70 mV, +30 mV, and +60 mV, respectively. In con-

Table 1: Boltzmann parameters of Ca^{2+} conductance, charge movements and Ca^{2+} transients of control, γ_1 het and γ_1 null myotubes.

CELL TYPE	G-V			Q-V		
	G_{max} (pS/pF)	$V_{1/2}$ (mV)	k (mV)	Q_{max} (fC/pF)	$V_{1/2}$ (mV)	k (mV)
Control, +/+	131 ± 6.2	14.7 ± 2.1	4.2 ± 0.4	5.3 ± 0.4	11.4 ± 2.5	15.4 ± 1.1
(n)	(8)			(8)		
γ_1 het, +/-	161 ± 11.5[a]	14.3 ± 2.8	5 ± 0.8	5.3 ± 0.3	14.4 ± 0.6	14.7 ± 2.0
(n)	(8)			(4)		
γ_1 null, -/-	170 ± 9.6[b]	10.9 ± 0.9	4.5 ± 0.4	5.3 ± 0.9	17.8 ± 1.9	15.8 ± 2.2
(n)	(12)			(8)		
	ΔF/Fo-V			**Inactivation**		
	$\Delta F/Fo_{(max)}$	$V_{1/2}$ (mV)	k (mV)		$V_{1/2}$ (mV)	k (mV)
Control, +/+	3.9 ± 0.3	4.6 ± 1.2	10.2 ± 1.3		-4.6 ± 3.6	7.3 ± 0.2
(n)	(6)				(6)	
γ_1 het, +/-	3.3 ± 0.5	8.2 ± 3.0	10.1 ± 2.0		8.1 ± 2.3[c]	8.0 ± 0.6
(n)	(4)				(8)	
γ_1 null, -/-	3.7 ± 0.4	7.3 ± 1.6	9.0 ± 1.1		8.9 ± 0.8[d]	8.1 ± 0.8
(n)	(6)				(8)	

Entries (mean ± SEM) correspond to Boltzmann parameters fitted to each cell (number of cells n, in parenthesis). The only statistically significant differences ($p<0.05$) were for either γ_1 het or γ_1 null cells compared to control cells as indicated. The t-test p values were 0.004, 0.009, 0.011, 0.009 for a-d, respectively.

trast, γ_1 het and γ_1 null cells showed less inactivation during the pre-pulse, and thus a significantly larger Ca^{2+} current during the test pulse. Furthermore, pre-pulse potentials larger than +30 mV did not promote additional inactivation, which can be seen by comparing traces 2 and 3 in the γ_1 het and γ_1 null cells. Fig. 3B shows the maximum Ca^{2+} current during the test pulse plotted as a function of the pre-pulse potential. In control cells, inactivation was complete when the pre-pulse potential was above +30 mV (-6.9 ± 0.8 pA/pF at -70 mV vs. -0.2 ± 0.2 pA/pF at +70 mV, n = 6 cells). In γ_1 null cells, inactivation reached a plateau when the pre-pulse potential was more positive than +20 mV (-8.5 ± 0.9 pA/pF at -70 mV vs. -3.2 ± 0.7 pA/pF at +70 mV, n = 8 cells). Incomplete inactivation was also seen in γ_1 het cells, although this was less pronounced than in γ_1 null cells. Since the pre-pulse was not sufficiently long for inactivation to reach steady-state, we are not certain whether the observed incomplete inactivation reflects a component of the γ_1 null Ca^{2+} current that inactivates extremely slowly or a "truly" non-inactivating component. To compare the voltage-dependence of the inactivation produced by the 2.5-second pre-pulse, the Ca^{2+} current during the test pulse was normalized and fit to the Boltzmann equation (Fig. 3C). The curves for γ_1 het and γ_1 null cells showed a significant ($p<0.05$) shift to more positive potentials compared to control cells. The same conclusion was reached by comparing the Boltzmann parameters of individual cells in Table 1. Since control cells had a more negative half inactivation potential, the higher Ca^{2+} conductance of γ_1 het and γ_1 null cells reported in Fig. 2 could be explained by a larger steady-state inactivation of the control Ca^{2+} current at the -40 mV holding potential. To determine if this was the case, we measured the Ca^{2+} conductance during the pre-pulse for the same cells analyzed in Fig 3B,C. The pre-pulse was delivered from a holding potential of -80 mV, and therefore the pre-pulse current should be less contaminated by steady-state inactivation. G_{max} at the peak of the Ca^{2+} current during the pre-pulse was 146 ± 12 pS/pF for controls, 172 ± 18 pS/pF γ_1 het and 186 ± 13 pS/pF for γ_1 null cells with t-test statistical significance for controls vs. γ_1 null cells of $p = 0.034$ and for controls vs. γ_1 het cells of $p = 0.064$. Thus the higher Ca^{2+} conductance of γ_1 het and γ_1 null

cells persisted at the more negative holding potential. These Ca^{2+} conductances were approximately 10% higher than those at the -40 mV holding potential reported in Table 1. The additional current could have been contributed by T-type Ca^{2+} channels (not shown), which are available at the -80 mV holding potential but are inactivated at the more positive holding potential. Also, since the T-type Ca^{2+} current density was highly variable (see above), this could explain the higher p values compared to those reported in Table 1. In summary, decreasing the amount of the γ_1 subunit protein or eliminating it completely resulted in myotubes with a higher Ca^{2+} current density, a similar voltage-dependence of activation, and a reduced rate of inactivation. These results, with the exception of the change in Ca^{2+} current density, are in remarkable agreement with those obtained when L-type Ca^{2+} channel subunits are coexpressed without the γ_1 subunit in heterologous cells (see below). They also are similar to results obtained elsewhere in γ_1 null myotubes using a 5-second pre-pulse [20]. Furthermore, the incomplete inactivation of the γ_1 null Ca^{2+} current resembles that observed in ts A201 cells expressing DHPRs specifically lacking γ_1 and using a 3-second inactivation protocol [22].

The effect of the γ_1 subunit on Ca^{2+} current kinetics has been somewhat confusing until now, because it has not been possible to examine its role using homologous subunits and a homologous expression system. In amphibian oocytes, γ_1 was assayed in a complex with α_{1C}, β_{1a} and α_2-δ [23,24]. These investigators found γ_1 produced a slight decrease in Ca^{2+} current density, no change in activation kinetics and a positive shift in the peak Ca^{2+} current vs. voltage curve. In HEK293 cells using the same subunit composition, the γ_1 subunit did not alter the kinetics or density of Ca^{2+} currents [25]. However, in both oocytes and HEK293 cells, the γ_1 subunit increased the rate of Ca^{2+} channel inactivation and produced a large hyperpolarizing shift in steady-state inactivation [23,25,26]. The results obtained here in skeletal muscle demonstrate that absence of the γ_1 subunit increases Ca^{2+} current density, decreases the inactivation rate, and shifts the voltage-dependence of inactivation in the depolarizing direction. Freise et al. [20] showed that the increase in Ca^{2+} current was not a result of changes in single channel conductance and suggested the effects were due to changes in channel open probability. However, this remains to be tested directly. Expression of the γ_2 subunit in BHK cells expressing α_{1A}, α_2-δ and β_{1a} also shifts the voltage-dependence of inactivation ~ 7 mV in the hyperpolarizing direction [17]. In summary, the two γ subunits that have been characterized to date, namely γ_1 in the homologous skeletal myotube system described here and γ_2 described above in heterologous BHK cells [17], appear to be inhibitory. In each case, the presence of γ results in fewer Ca^{2+} channels available for activation.

Absence of changes in the EC coupling voltage sensor of γ_1 nullmyotubes

The impact of the γ_1 null mutation on myotube EC coupling was inferred from intramembrane charge movements, the bulk of which have been shown to originate from the DHPR voltage sensor [27,28]. Additionally, we measured Ca^{2+} transients evoked by voltage (i.e., by the movement of the voltage sensor) and compared these two sets of data. To measure DHPR charge movements and to separate these charge movements from those produced by other voltage-gated channels, a) ionic currents were blocked; b) the linear component of the cell capacity was subtracted using a P/4 procedure and by analog compensation; and c) we used a pulse protocol that eliminated the immobilization-sensitive charge movements from voltage-gated Na^+ channels and presumably also from T-type Ca^{2+} channels. Previous studies in dysgenic (α_{1S} null) myotubes transfected with α_{1S} showed that the pulse protocol and the internal and external solutions used here (see Materials and Methods) detected charge movements of a magnitude 5 to 8 fold larger than those present in non-transfected dysgenic myotubes [28]. Thus we are confident that the technique adequately measures intramembrane charge movements in DHPR voltage sensors present in the plasma membrane. Fig. 4A shows "gating-type" currents produced by charge movements in response to 3 of 14 step voltages delivered to each cell (-40, +10, and +70 mV). Charge movements did not occur at -40 mV in any of the cell types. Traces at +10 mV and +70 mV show a transient current at the onset of the voltage step, the ON charge, and an equal inverted current at the end of the voltage step, the OFF charge. The voltage-dependence of the OFF charge estimated by integration is shown in Fig. 4B. The OFF transient was usually less contaminated by ionic current than the ON transient, and for that reason it provides a better estimate of the total DHPR charge. The main contaminant of the ON transient was a non-linear outward current, presumably a K^+ channel that was not always completely blocked by the pipette solution. The OFF charge increased in a sigmoidal fashion and saturated at potentials more positive than +60 mV in all cases. These data were adequately fit by a Boltzmann equation shown by the lines. We found that the fitted maximum charge (Q_{max}) expressed by the 3 cell types was ~ 5 fC/pF, in agreement with previous determinations in normal myotubes [29]. Furthermore, Boltzmann parameters determined for each cell and then averaged were not significantly different in any of two-by-two comparisons between control, γ_1 het or γ_1 null cells (Table 1). In summary, the magnitude of intramembrane charge movements and its voltage dependence were unaltered by

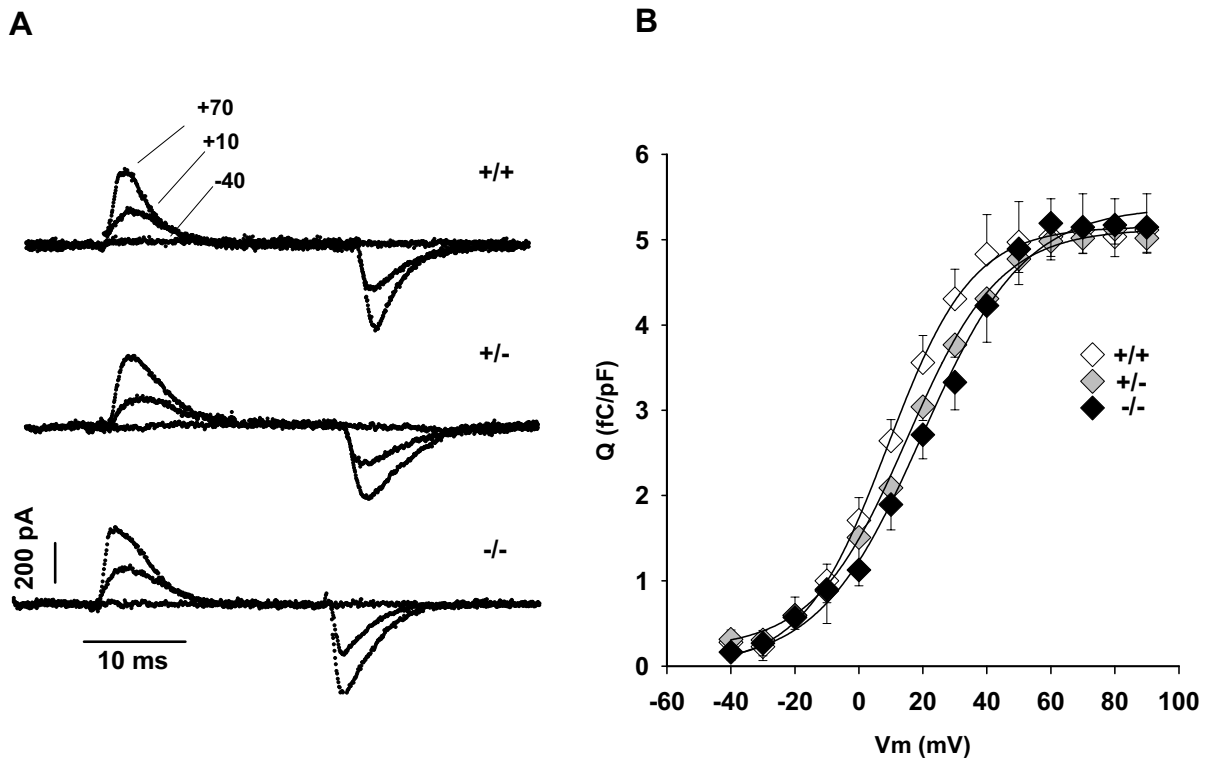

Figure 4
Voltage dependence of intramembrane charge movements in γ_1 knockout myotubes. A) Whole-cell current produced by charge movements in response to 3 of 14 25-ms voltage steps delivered to the same cell. The voltage steps shown are to -40 mV, +10 mV, and +70 mV. The cell capacitance was 241 pF for the control, 292 pF for the γ_1 het and 253 pF for the γ_1 null cell. B) Voltage dependence of charge movement obtained by integration of the OFF transient current for 8 control, 4 γ_1 het, and 8 γ_1 null cells. The curves correspond to a Boltzmann fit of the population mean with the following parameters. Q_{max} = 5.2 fC/pF, $V_{1/2}$ = 13.2 mV and k = 9 mV for control cells. Q_{max} = 4.9 fC/pF; $V_{1/2}$ = 15 mV and k = 14.5 mV for γ_1 het cells. Q_{max} = 5.4 fC/pF, $V_{1/2}$ = 19.6 mV and k = 16 mV for γ_1 null cells.

partial or complete removal of the γ_1 subunit. Furthermore, in agreement with previous data [29], no additional charges moved when pulses were delivered from a holding potential of -120 mV (data not shown). Thus, failure to detect changes in the charge vs. voltage characteristics of γ_1 null myotubes compared to controls cannot be explained by charge movements in the γ_1 null myotubes occurring at potentials more negative than the chosen -80 mV holding potential.

Absence of alterations in the voltage dependence of charge movement in the γ_1 null cells should also be reflected in the voltage-dependence of Ca^{2+} transients. Changes in intracellular Ca^{2+} were measured using confocal line-scan imaging of fluo-4 fluorescence. Fig. 5A shows a line-scan image of a Ca^{2+} transient stimulated by a 50 ms depolarization to +90 mV from a holding potential of -40 mV in each cell type. The scan direction was perpendicular to the long axis of the myotube in a region selected on the basis of a low resting fluorescence and a high stimulated fluorescence (red/yellow color). The two traces on top of each image correspond to the time course of the fluo-4 fluorescence averaged across the entire line-scan at -10 mV, which is close to the threshold, and at +90 mV, which produced the maximum Ca^{2+} transient. Increase in cytosolic Ca^{2+} started at the onset of the depolarization and peaked ~ 100 ms later in the three cell types. For all cells, the peak fluorescence change for the depolarization to +90 mV was >3 $\Delta F/Fo$ units, which is equivalent to >4 times the resting fluorescence. The relatively long recovery time following the depolarization is due to the low Ca^{2+} buffering power of the internal recording solution and is in agreement with previous studies [27,30]. The voltage dependence of $\Delta F/Fo$

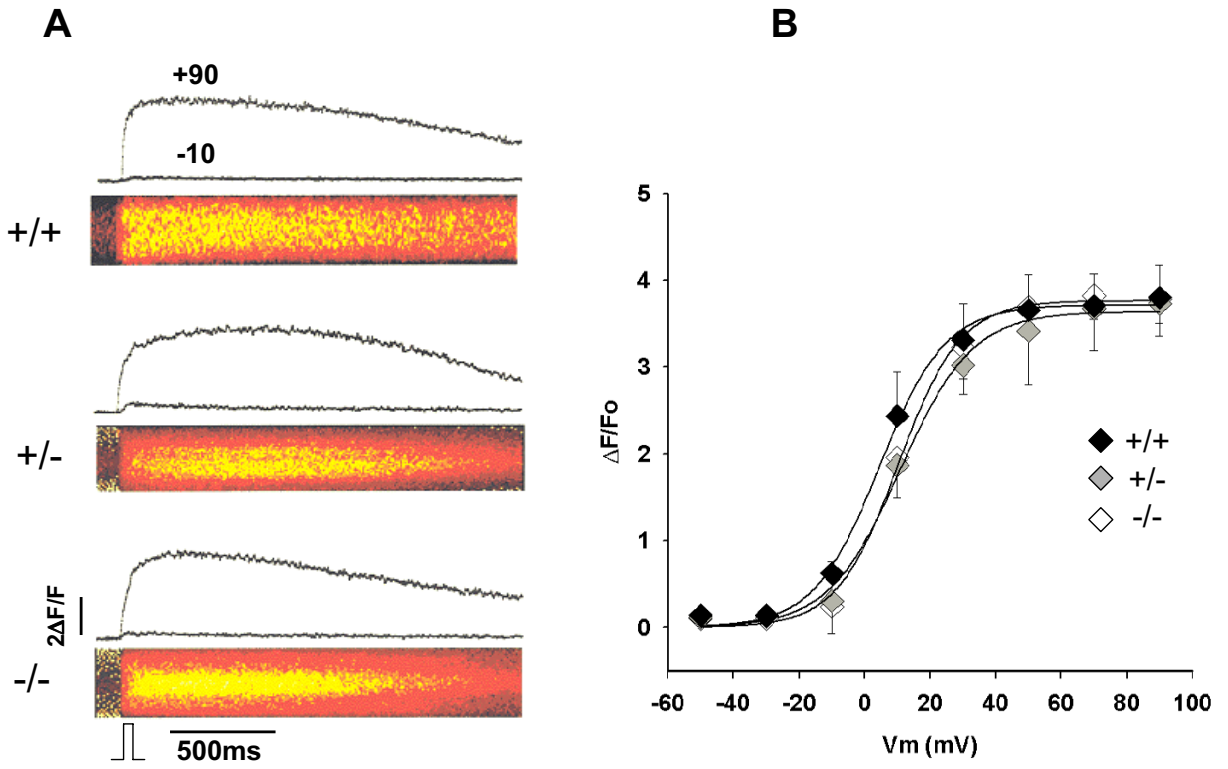

Figure 5

Voltage-dependence of Ca^{2+} transients in γ_1 knockout and normal myotubes. A) Confocal line-scan images of fluo-4 fluorescence in response to a 50 ms step to +90 mV from a holding potential of -40 mV. Hot colors represent high fluorescence (yellow>red). The pulse was delivered 100 ms after the start of the line-scan as indicated at the bottom of the figure. Images have a horizontal dimension of 2.05 seconds in all cases. The vertical dimension was 15, 28, and 24 microns for the control, γ_1 het, and γ_1 null cells, respectively. The two curves on top of the image show the time course of the fluorescence intensity at -10 mV and +90 mV. 1 ΔF/Fo unit corresponds to a doubling of the cell resting fluorescence. B) Voltage-dependence of the peak ΔF/Fo for 6 control, 4 γ_1 het, and 6 γ_1 null cells. The curves correspond to a Boltzmann fit of the population mean with the following parameters. $\Delta F/Fo_{max}$ = 3.8, $V_{1/2}$ = 10 mV, k = 9.4 mV for control cells. $\Delta F/Fo_{max}$ = 3.6, $V_{1/2}$ = 10.8 mV; k = 10.9 mV for γ_1 het cells. $\Delta F/Fo_{max}$ = 3.7, $V_{1/2}$ = 4.5 mV; k = 10 mV for γ_1 null cells.

measured at the peak of the transient is shown in Fig. 5B. All curves had the same profile which consisted of a threshold for peak Ca^{2+} release at -10 mV, an increase in peak Ca^{2+} with pulse potential from -10 mV to +30 mV and a plateau at more positive potentials. Furthermore, two-by-two comparisons of Boltzmann parameters fitted to each cell did not reveal statistically significant differences (see Table 1). In summary, the voltage-dependence of Ca^{2+} transients and the maximum cytosolic Ca^{2+} concentration during the transient were not significantly affected by partial or total absence of the γ_1 subunit. However, we cannot rule out changes in the rate of SR Ca^{2+} release since this measurement requires an entirely different internal solution [31]. A recent report indicates that the SR Ca^{2+} release rate is slightly higher in γ_1 null myotubes [32].

Involvement of DHPR subunits in voltage sensing and EC coupling

The α_{1S} pore subunit of the skeletal DHPR is the main determinant of charge movements and EC coupling [4,27,28]. However, other subunits of the DHPR are critical modulators of both functions. In heterologous expression systems, the α_2-δ subunit was shown to affect the rate of Ca^{2+} current inactivation and charge movement immobilization [33]. Studies investigating the role of the β subunit on charge movement vary with the expression system used. In amphibian oocytes, β subunits increase the coupling between charge movements and

channel opening [34,35]. We have shown in skeletal muscle cells lacking the β_1 subunit that reintroduction of variants of β_1 has little effect on either charge movement or the kinetics of activation of the expressed Ca^{2+} current [15]. However, the carboxyl terminus of β1a is an important determinant of the efficiency of the coupling between charge movement and Ca^{2+} release [15]. In contrast to these results, earlier studies in which similar β subunits were co-expressed with α_1 subunits in oocytes indicated β subunits had major effects on Ca^{2+} current density and gating kinetics [36,37]. While the reason for these discrepancies is unknown, they highlight the fact that in skeletal muscle, the gating characteristics of the L-type Ca^{2+} channel might be controlled by interactions beyond those taking place among subunits of the DHPR. For example, a region of RyR1 has been shown to be essential for L-type Ca^{2+} current expression [38]. Such interaction is critical for skeletal DHPR function and is unlikely to occur in heterologous expression systems.

Conclusions

The ability of the γ_1 subunit to selectively modulate the pore function of the DHPR without modulation of charge movements or the voltage dependence of Ca^{2+} transients is unique, especially since other DHPR subunits participate in both functions. In all likelihood, the charge movement protocol failed to detect gating currents responsible for opening the Ca^{2+} channel, which are quite small and are only resolved for depolarizations >200 ms [39] compared to the 25 ms used here (Fig. 4). A possible shift in the voltage-dependence of these charges recruited by long depolarizations would be consistent with the shift in Ca^{2+} current inactivation and remains to be resolved in γ_1 null myotubes. However, the protocol accurately measures the immobilization-resistant charge movements that are known to be required for skeletal-type EC coupling [31,40]. Therefore, the γ_1 subunit is unlikely to play a critical role in the activation of SR Ca^{2+} release, in agreement with a recent report [32]. However, shifts in voltage dependence below the limit of resolution (see Materials and Methods) and effects on charge movement and Ca^{2+} release inactivation cannot be completely ruled out. The γ_1 knockout mice provide a unique resource to understand the function of this protein in myotubes in molecular detail.

Materials and Methods

Gene targeting

Bacteriophage clones containing portions of the γ_1 gene were isolated from a mouse 129Sv genomic library (Stratagene, La Jolla, CA #946305). To inactivate the γ_1 gene, a 4.4 kb *Bam*HI/*Xho*I fragment upstream of exon 1 was subcloned into a multiple cloning site 5' of the *neo* and Herpes virus TK gene that was in pBluescript (Stratagene). A second 2.6 kb *EcoR*I/*BamH*I fragment 3' of exon 4 of the γ_1 gene was cloned into a site between the *neo* and TK genes (Fig. 1Aii). Thus, the targeting vector contains 4.4 kb of identity with the native γ_1 gene 5', and 2.6 kb of identity 3' of the *neo* cassette, respectively. The targeting vector also contains the HSV TK gene to allow for negative selection of non-recombinants. A unique *Bam*HI restriction site was used to linearize the plasmid prior to its introduction into mouse ES cells by electroporation. The γ_1 gene contains 4 exons, and correct targeting results in the deletion of all 4 exons, which will inactivate the gene (Fig. 1Aiii). Probe 2 was used for identification of targeted clones [41]. 5 μg of the targeting vector was electroporated into 5×10^6 AB1 ES cells. G418 and FIAU (1-(2'-deoxy-2'-fluoro-γ-D-arabinofuranosyl)-5-iodouracil) resistant clones were analyzed by Southern blotting after digestion with either *Eco*RI and hybridization to probe 1 or digestion with *Hind*III and hybridization to probe 2 (Fig. 1). Of three clones targeted on the 5' end, two also were targeted on the 3' end. These were expanded and used to produce germline chimeras. Mice homozygous for the targeted allele were viable, with no apparent abnormalities. Mice heterozygous and homozygous for the targeted mutation are referred to as γ_1 het and γ_1 null, respectively.

Western blots

Total microsomes were prepared from the forelimb and hind limb muscles of control, γ_1 het, and γ_1 null adult mice as previously described [42]. Total microsomes were washed twice with 0.6 M KCl buffer and 100 μg of total membrane protein was applied to a 5-15% SDS polyacrylamide gel. Proteins were transferred to PVDF membranes and analyzed with either anti-α_{1S} mAb IIC12 antibody [43], or anti-α_2-δ protein G-purified guinea pig antibody #1 [13], or anti-β_{1a} affinity-purified sheep #6 antibody [44], or with anti-γ_1 affinity-purified guinea pig #16 antibody and the appropriate secondary antibodies [11]. The subunits were visualized using SuperSignal ECL reagent (Pierce, Rockford, IL). The images were captured on a Chemi-Imager (Alpha Innotech, San Leandro, CA) set to a level just below saturation.

Primary cultures of mouse myotubes

Primary cultures were prepared from hind limbs of day 18 embryos (E18) as described previously [45]. Dissected muscles were incubated for 9 min at 37°C in Ca^{2+}/Mg^{2+}-free Hanks balanced salt solution (in mM: 136.9 NaCl, 3 KCl, 0.44 KH_2PO_4, 0.34 $NaHPO_4$, 4.2 $NaHCO_3$, 5.5 glucose, pH 7.2) containing 0.25% (w/v) trypsin and 0.05 % (w/v) pancreatin (Sigma, St. Louis, MO). Mononucleated cells were resuspended in plating medium containing 78% Dulbecco's modified Eagle's medium (DMEM) with low glucose (Life Technologies, Rockville, MD), 10 % horse serum (HS, Sigma, St. Louis, MO), 10 % fetal bovine serum (FBS, Sigma, St. Louis, MO), 2% chicken em-

bryo extract (CEE, Life Technologies, Rockville, MD) and plated on plastic culture dishes coated with gelatin at a density of ~ 1×10^4 cells per dish. Cultures were grown at 37°C in 8 % CO_2. After the fusion of myoblasts (~ 7 days), the medium was replaced with a FBS-free medium (88.75 % DMEM, 10 % HS, 1.25% CEE) and cells were incubated in 5% CO_2. All media contained 0.1 % v/v penicillin and streptomycin (Sigma, St. Louis, MO). All measurements were made when the cells had been in culture for 7-10 days. During this time the maximal current density did not change [45].

Electrophysiological measurements

Whole-cell recordings were performed as described previously [29] using an Axopatch 200B amplifier (Axon Instruments, Foster City, CA). Linear capacity and leak currents were compensated with the circuit provided by the manufacturer. Series resistance, Rs, was compensated up to the point of amplifier oscillation with the Axopatch circuit. Considering all cells in the present study, the linear capacitance (mean ± SE) of control, γ_1 null, and γ_1 het myotubes was 256 ± 25 pF (38 cells), 246 ± 16 pF (34 cells) and 223 ± 24 (23 cells), respectively. Rs of the same cells before analog compensation was 7 ± 0.5 MΩ, 7.2 ± 0.4 MΩ, and 6.3 ± 0.5 MΩ, respectively. Following compensation, the effective Rs was <2 MΩ in all cases measured, although this was not measured systematically. Considering a mean cell capacitance of 240 pF, a typical maximum current density of 5 to 10 pA/pF (see Fig. 3B), and Rs (effective)<2 MΩ, the voltage error was <2.4 to <4.8 mV. All experiments were performed at room temperature. Patch pipettes had an open tip resistance of 1-2 MΩ when filled with the pipette solution. Ca^{2+} currents were measured from a holding potential of -40 mV. Test pulses of 500 ms in 5 mV increments ranged from -40 mV to +60 mV. Ca^{2+} conductance vs. voltage curves were obtained by extrapolation of the Ca^{2+} current to the reversal potential of the cell. To measure inactivation, cells were held at -80 mV, then stepped to a series of depolarizing (pre-pulse) voltages, from -70 mV to +70 mV in 10 mV increments, for 2.5 seconds to promote inactivation, then stepped to -50 mV for 100 ms to close non-inactivated channels, then stepped for 200 ms to the test potential of +20 mV to measure Ca^{2+} currents, then stepped to the -80 mV holding potential for 5 seconds to permit recovery from inactivation. Charge movement was measured using a protocol that eliminated immobilization-sensitive components [15,28,29]. Voltage was stepped from a holding potential of -80 mV to -35 mV for 750 ms, then to -50 mV for 5 ms, then to test potential for 25 ms, then to -50 mV for 30 ms and finally to the -80 mV holding potential. Subtraction of the linear component was assisted by a P/4 procedure following the pulse paradigm listed above. P/4 pulses were separated by 500 ms and had a duration of 25 ms. Previous studies showed this choice of pulse protocol and internal and external solutions resulted in nifedipine-sensitive charge movements of a magnitude ~ 5 fold larger than those detected in dysgenic myotubes lacking α_{1S} [29].

Solutions

The external solution in all cases was (in mM) 130 TEA methanesulfonate, 10 $CaCl_2$, 1 $MgCl_2$, 10 HEPES titrated with TEA(OH) to pH 7.4. For Ca^{2+} transients and Ca^{2+} currents, the pipette solution was (in mM) 140 Ca^{2+}-Aspartate, 5 $MgCl_2$, 0.1 EGTA (Ca^{2+} transients) or 5 mM EGTA (Ca^{2+} currents), and 10 MOPS-CsOH pH 7.2. For charge movements, the pipette solution was (in mM) 120 NMG (N-methyl glucamine)-Glutamate, 10 HEPES-NMG, 10 EGTA-NMG pH 7.3. For charge movements, the external solution was supplemented with 0.5 mM $CdCl_2$ and 0.5 mM $LaCl_3$ to block the Ca^{2+} current and 0.05 mM TTX to block residual Na^+ current.

Ca^{2+} transient measurements

Ca^{2+} transients were measured using a confocal microscope in line-scan mode as described previously [46,47,48]. Cells were loaded with 4 mM fluo-4 (fluo-4 acetoxymethyl (AM) ester, Molecular Probes, Eugene, OR) for 20 to 40 min at room temperature. Stocks of fluo-4 (1 mg/ml) were made in DMSO and stored frozen. All experiments were performed at room temperature. Cells were viewed with an inverted Olympus microscope with a 20X objective (N.A. = 0.4) and a Fluoview confocal attachment (Olympus, Melville, NY). The 488 nm spectrum line necessary for fluo-4 excitation was provided by a 5 mW argon laser attenuated to 20% with neutral density filters. The fluorescence intensity, F, was calculated by densitometric scanning of line-scan images and was averaged over the entire width of the cell. The background fluorescence intensity (Fo) was averaged in the same manner from areas of the same image prior to the voltage pulse. The fluorescence unit $\Delta F/Fo$ corresponds to (F-Fo)/Fo. The limit of fluorescence detection, based on microscope settings and the average resting fluo-4 fluorescence, was ~ 0.1 $\Delta F/Fo$ units. That is, we could detect a ~ 10% change above the cell resting fluorescence. Using a pseudo-ratiometric equation for estimating the cytosolic free Ca^{2+} [48] and assuming a resting free Ca^{2+} of 100 nM [48], the nominal limit of resolution of free Ca^{2+} change was ~ 200 nM.

Data and error analysis

For each cell, or for the population average, the voltage dependence of charge movements (Q), Ca^{2+} conductance (G), and peak intracellular Ca^{2+} ($\Delta F/Fo$) were fitted according to a Boltzmann equation $A = A_{max}/(1+\exp(-(V-V_{1/2})/k))$ where A_{max} was either Q_{max}, G_{max} or $\Delta F/Fo_{max}$; $V_{1/2}$ is the potential at which $A = A_{max}/2$; and k is the slope factor. For a fit of steady-state inactivation, the

term ($V-V_{1/2}$) in the equation above was replaced by ($V_{1/2}-V$). Ca^{2+} conductance for each cell was computed from the extrapolated reversal potential and the maximal Ca^{2+} current at each voltage. In all figures, the symbols and error bars correspond to the population mean ± 1 SEM. The curves correspond to a Boltzmann fit of the mean. In addition to Student t-tests reported in Table 1, one-way ANOVA tests were conducted among the 11 sets of Boltzmann parameters of control, γ_1 het and γ_1 null cells of Table 1. The null hypothesis (equality of means) was not rejected at a level of significance $p<0.05$ except in the two cases also identified by t-tests, namely G_{max} and $V_{1/2}$ inactivation. An F-test, which formally tests for the difference between the variances of independent populations, was used to determine which of the fitted Boltzmann parameters (A_{max}, $V_{1/2}$, k) had the largest variance, and thus the largest experimental error. The ranking order in variance error was $V_{1/2}>A_{max}>k$. Furthermore, the error in $V_{1/2}$ was the largest for the fluorescence measurement and the smallest for the conductance measurement. This result was expected since the size of the voltage step used in the $V_{1/2}$ determination was 5 mV for conductance, 10 mV for charge movements, and 20 mV for fluorescence. The number of voltage steps in fluorescence measurements was kept to a minimum to avoid rundown of the Ca^{2+} transient due to photobleaching. The limit of resolution of $V_{1/2}$, the parameter with the largest error, was estimated with a z-test which formally tests for the difference between the mean of a population and a hypothetical mean. We determined the smallest difference between a experimental and a hypothesized $V_{1/2}$ resolvable at a level of statistical confidence $p<0.05$. In the calculations, we used the data with the largest $V_{1/2}$ variance for each measurement (conductance, charge movement and fluorescence). Also, we assumed a hypothetical S.D. equal to the experimental S.D. The estimated limits of statistical resolution were ~ 3.9 mV for conductance, ~ 6.5 mV for charge movements, and ~ 8.5 mV for fluorescence measurements. Thus, a difference in population mean $V_{1/2}$ of less than the indicated limit would not be statistically significant, given the variance and the number of determinations of the present study. Statistical analyses were performed with Analyse-it software (Leeds, UK)

List of Abbreviations

AID (α subunit interaction domain); BID (β subunit interaction domain); DMSO (dimethyl sulfoxide); EGTA (ethylene glycol bis-aminoethylether tetraacetic acid); HEPES (2-hydroxylethyl piperazine 2-ethane sulfonic acid); MOPS (3N-Morpholino-propane sulfonic acid); PVDF (polyvinylidene difluoride); TTX (tetrodotoxin); TEA (tetraethylamonium).

Acknowledgements

Supported by National Institutes of Health Grant HL-47053 (R.C, P.A.P., and R.G.G.), AR46448 (R.C.), National Science Foundation IBN-9319540 (R.G.G. and P.A.P) and by a predoctoral fellowship from Wisconsin Heart Association (C.A.A). K.P.C. is an investigator of the Howard Hughes Medical Institute.

References

1. Perez-Reyes E, Schneider T: **Calcium channels: Structure, Function, and Classification.** *Drug Dev Res* 1994, **33**:295-318
2. McPherson PS, Campbell KP: **The ryanodine receptor/Ca2+ release channel.** *J Biol Chem* 1993, **268**:13765-13768
3. Rios E, Pizarro G: **Voltage sensor of excitation-contraction coupling in skeletal muscle.** *Physiol Revs* 1991, **71**:849-908
4. Tanabe T, Beam KG, Adams BA, Niidome T, Numa S: **Regions of the skeletal muscle dihydropyridine receptor critical for excitation-contraction coupling.** *Nature* 1990, **346**:567-572
5. Nakai J, Tanabe T, Konno T, Adams B, Beam KG: **Localization in the II-III loop of the dihydropyridine receptor of a sequence critical for excitation-contraction coupling.** *J Biol Chem* 1998, **273**:24983-24986
6. Pragnell M, DeWaard M, Mori Y, Tanabe T, Snutch TP, Campbell KP: **Calcium channel β-subunit binds to a conserved motif in the I-II cytoplasmic linker of the α1 -subunit.** *Nature* 1994, **368**:67-70
7. De Waard M, Pragnell M, Campbell KP: **Ca2+ channel regulation by a conserved β subunit domain.** *Neuron* 1994, **13**:495-503
8. Birnbaumer L, Qin N, Olcese R, Tareilus E, Platano D, Costantin D, Stefani E: **Structures and functions of calcium channel β subunits.** *J Bioenereg Biomemb* 1998, **30**:357-375
9. Gurnett CA, Campbell KP: **Transmembrane auxiliary subunits of voltage-dependent ion channels.** *J Biol Chem* 1996, **271**:27975-27978
10. Gurnett CA, De Waard M, Campbell KP: **Dual function of the voltage-dependent Ca2+ channel α2-δ subunit in current stimulation and subunit interaction.** *Neuron* 1996, **16**:431-440
11. Sharp AH, Campbell KP: **Characterization of the 1,4 dihydropyridine receptor using subunit-specific polyclonal antibodies: evidence of a 32,000-Da subunit.** *J Biol Chem* 1989, **264**:2816-2825
12. Jay SD, Ellis SB, McCue AF, Williams ME, Vedvick TS, Harpold MM, Campbell KP: **Primary structure of the γ subunit of the L-type calcium channel from rabbit skeletal muscle.** *Science* 1990, **248**:490-492
13. Bosse E, Regulla S, Biel M, Ruth P, Meyer HE, Flockerzi V, Hofmann F: **The cDNA and deduced amino acid sequence of the γ subunit of the L-type calcium channel from rabbit skeletal muscle.** *FEBS Letters* 1990, **267**:153-156
14. Gregg RG, Messing A, Strube C, Beurg M, Moss R, Behan M, Sukhareva M, Haynes S, Powell JA, Coronado R, Powers PA: **Absence of the β subunit (cchb1) of the skeletal muscle dihydropyridine receptor alters expression of the α1 subunit and eliminates excitation-contraction coupling.** *Proc Natl Acad Sci USA* 1996, **93**:13961-13966
15. Beurg M, Ahern CA, Vallejo P, Conklin MW, Powers PA, Gregg RG, Coronado R: **Involvement of the carboxy-terminus region of the dihydropyridine receptor β1a subunit in excitation-contraction coupling of skeletal muscle.** *Biophys J* 1999, **77**:2953-2967
16. Qin N, Olcese R, Stefani E, Birnbaumer L: **Modulation of human neuronal α1E-type calcium channel by α2-δ subunit.** *Am J Physiol* 1998, **274**:C1324-C1331
17. Letts VA, Felix R, Biddlecome GH, Arikkath J, Mahaffey CL, Valenzuela A, Bartlett FS, Mori Y, Campbell KP, Frankel WN: **The mouse stargazer gene encodes a neuronal Ca2+ channel γ subunit.** *Nature Genet* 1998, **19**:340-347
18. Klugbauer N, Dai S, Specht V, Lacinova L, Marais E, Bohn G, Hofmann F: **A family of γ-like calcium channel subunits.** *FEBS Lett* 2000, **470**:189-197
19. Burgess DL, Gefrides LA, Foreman PJ, Noebels JL: **A cluster of three novel Ca2+ channel γ subunit genes in chromosome 19q13.4: Evolution and expression profile of the γ subunit family.** *Genomics* 2001, **71**:339-350
20. Freise D, Held B, Wissenbach U, Pfeifer A, Trost C, Himmerkus N, Schweig U, Freichel M, Biel M, Hofmann F, Hoth M, Flockerzi V: **In-**

activation properties and current densities of skeletal muscle L-type calcium channel are altered in γ1 deficient mice. *J Biol Chem* 2000, **275**:14476-14481
21. Morrill JA, Brown RH Jr, Cannon SC: **Gating of the L-type Ca2+ channel in human skeletal myotubes: An activation defect caused by the hypokalemic periodic paralysis mutation R528H.** *J Neurosci* 1998, **18**:10320-10334
22. Sipos I, Pika-Hartlaub U, Hofmann F, Flucher BE, Melzer W: **Effects of the dihydropyridine receptor subunits gamma and alpha2delta on the kinetics of heterologously expressed L-type Ca2+ channels.** *Pflugers Arch* 2000, **439**:691-699
23. Singer D, Biel M, Lotan I, Flockerzi V, Hofmann F, Dascal N: **The roles of the subunits in the function of the calcium channel.** *Science* 1991, **253**:1553-1557
24. Wei X, Perez-Reyes E, Lacerda AE, Schuster G, Brown AM, Birnbaumer L: **Heterologous regulation of the cardiac Ca2+ channel α1 subunit by skeletal muscle β and γ subunits.** *J Biol Chem* 1991, **266**:21943-21947
25. Lerche H, Klugbauer N, Lehmann-Horn F, Hofmann F, Melzer W: **Expression and functional characterization of the cardiac L-type calcium channel carrying a skeletal muscle DHP receptor mutation causing hypokalaemic periodic paralysis.** *Pflugers Arch* 1996, **431**:461-463
26. Eberst R, Dai S, Klugbauer N, Hofmann F: **Identification and functional characterization of a calcium channel γ subunit.** *Pflugers Arch* 1987, **433**:633-637
27. Garcia J, Beam KG: **Relationship of calcium transients to calcium currents and charge movements in myotubes expressing skeletal and cardiac dihydropyridine receptors.** *J Gen Physiol* 1994, **103**:125-147
28. Ahern CA, Arikkath J, Vallejo P, Gurnett CA, Powers PA, Campbell KP, Coronado R: **Intramembrane charge movements and excitation-contraction coupling expressed by two-domain fragments of the Ca2+ channel.** *Proc Natl Acad Sci USA* 2001, **98**:6935-6940
29. Strube C, Beurg M, Powers PA, Gregg RG, Coronado R: **Reduced Ca2+ current, charge movement and absence of Ca2+ transients in skeletal muscle deficient in dihydropyridine receptor** *Biophys J* 1996, **71**:2531-2543
30. Beurg M, Sukhareva M, Ahern CA, Conklin MW, Perez-Reyes E, Powers PA, Gregg RG, Coronado R: **Differential control of skeletal muscle Ca2+ current and excitation-contraction coupling by the dihydropyridine receptor β subunit.** *Biophys J* 1999, **76**:1744-1756
31. Melzer W, Schneider MF, Simon BJ, Szucs G: **Intramembrane charge movement and calcium release in frog skeletal muscle.** *J Physiol (Lond)* 1986, **373**:481-511
32. Ursu D, Sebille S, Dietze B, Freise D, Flockerzi V, Melzer W: **Excitation-contraction coupling in skeletal muscle of a transgenic mouse lacking lacking the dihydropyridine receptor subunit gamma1.** *J Physiol (Lond)* 2001, **533**:367-377
33. Shirokov R, Ferreira G, Yi J, Rios E: **Inactivation of gating currents of L-type calcium channels. Specific role of the α2δ subunit.** *J Gen Physiol* 1998, **111**:807-823
34. Neely A, Wei X, Olcese R, Birnbaumer L, Stefani E: **Potentiation by the β subunit of the ratio of the ionic current to the charge movement in the cardiac calcium channel.** *Science* 1993, **262**:575-578
35. Neely A, Olcese R, Baldelli P, Wei X, Birnbaumer L, Stefani E: **Dual activation of the cardiac Ca2+ channel 1C-subunit and its modulation by the β-subunit.** *Am J Physiol Cell Physiol* 1995, **268**:C732-C740
36. Olcese R, Qin N, Schneider T, Neely A, Wei X, Stefani E, Birnbaumer L: **The amino terminus of a calcium channel β subunit sets rates of channel inactivation independently of the subunit s effect on activation.** *Neuron* 1994, **13**:1433-1438
37. Qin N, Olcese R, Zhou JM, Cabello OA, Birnbaumer L, Stefani LE: **Identification of a second region of the β-subunit involved in regulation of calcium channel inactivation.** *Am J Physiol Cell Physiol* 1996, **271**:C1539-C1545
38. Nakai J, Sekiguchi N, Rando TA, Allen PD, Beam KG: **Two regions of the ryanodine receptor involved in coupling with L-type Ca2+ channels.** *J Biol Chem* 1998, **273**:13403-13406
39. Dirksen RT, Beam KG: **Role of calcium permeation in dihydropyridine receptor function. Insights into channel gating and excitation-contraction coupling.** *J Gen Physiol* 1999, **114**:393-403
40. Schneider MF, Chandler WK: **Voltage-dependent charge movement in skeletal muscle: a possible step in excitation-contraction coupling.** *Nature* 1973, **242**:244-246
41. Ramírez-Solis R, Davis AC, Bradley A: **Gene targeting in embryonic stem cells.** *Methods Enzymol* 1993, **225**:855-878
42. Witcher DR, De Waard M, Kahl SD, Campbell KP: **Purification and reconstitution of the N-type calcium channel complex from rabbit brain.** *Methods Enzymol* 1994, **238**:335-348
43. Leung AT, Imagawa T, Campbell KP: **Structural characterization of the 1,4 dihydropyridine receptor of the voltage-dependent Ca2+ channel from rabbit skeletal muscle: evidence for two distinct high molecular weight subunits.** *J Biol Chem* 1987, **262**:7943-7946
44. Pragnell M, Sakamoto J, Jay SD, Campbell KP: **Cloning and tissue-specific expression of the brain calcium channel β-subunit.** *FEBS Lett.* 1991, **291**:253-258
45. Beurg M, Sukhareva M, Strube C, Powers PA, Gregg RG, Coronado R: **Recovery of Ca2+ current, charge movements, and Ca2+ transients in myotubes deficient in dihydropyridine receptor β1 subunit transfected with β1 cDNA.** *Biophys J* 1997, **73**:807-818
46. Conklin MW, Ahern CA, Vallejo P, Sorrentino V, Takeshima H, Coronado R: **Comparison of Ca2+ sparks produced independently by two ryanodine receptor isoforms (type-1 or type-3).** *Biophys J* 2000, **78**:1777-1785
47. Conklin MW, Barone V, Sorrentino V, Coronado R: **Contribution of ryanodine receptor type-3 to Ca2+ sparks in embryonic mouse skeletal muscle.** *Biophys J* 1999, **77**:1394-1403
48. Conklin MW, Powers PA, Gregg RG, Coronado R: **Ca2+ sparks in embryonic mouse skeletal muscle selectively deficient in dihydropyridine receptor α1S or β1 subunits.** *Biophys J* 1999, **76**:657-669